J Electroceram (2012) 28:191–196
DOI 10.1007/s10832-012-9705-8

Synthesis and microwave dielectric properties of columbite-structure $MgNb_2O_6$ ceramics by aqueous sol–gel technique

H. T. Wu · Y. S. Jiang · W. B. Wu · F. Yang · Y. L. Yue

Received: 7 October 2011 / Accepted: 5 March 2012 / Published online: 18 March 2012

Abstract Columbite-type $MgNb_2O_6$ ceramics were prepared by aqueous sol–gel method and their microwave dielectric properties were investigated. Firstly, highly reactive nanosized $MgNb_2O_6$ powders were successfully synthesized at 500 °C in oxygen atmosphere with particle size of 20–40 nm. Phase formation was detected by DTA-TG and XRD. Subsequently, Sintering characteristics and microwave dielectric properties of $MgNb_2O_6$ ceramics were studied at different temperatures ranging from 1050 °C to 1250 °C. With the increase of sintering temperature, density, ε_r and $Q\times f$ values increased and saturated at 1150 °C with excellent microwave properties of ε_r=18.7, $Q\times f$= 90,700 GHz and τ_f=−48.5 ppm/°C. These results showed that the sintering temperature of $MgNb_2O_6$ ceramics was significantly reduced by aqueous sol–gel process.

Keywords $MgNb_2O_6$ · Nanopowder Synthesis · Sol–gel Process · Microwave Dielectric Properties

1 Introduction

The rapid progress in mobile and satellite communication system were creating high demands for the development of microwave dielectric materials with a high quality factor, an appropriate dielectric constant, and a near-zero temperature coefficient of resonant frequency. The columbite-like phase of magnesium niobate ($MgNb_2O_6$; MN) with a high $Q\times f$ value was considered as suitable material for microwave applications such as substrates and resonators at high frequency due to their low dielectric loss and high dielectric constant [1]. The present research about MN phase and its solid solution with magnesium tantalate phase prepared by conventional solid-state method were reported elsewhere [2–4] and the MN ceramic was investigated with excellent microwave properties of ε_r ~20, $Q\times f$ ~90,000 GHz and τ_f ~−68 ppm/°C at a sintering temperature region of as high as 1300~1450 °C/4 h [4]. Obviously high sintering temperatures of ceramics would limit their applications for practical cases, so the reduction of sintering temperature was desirable to enable commercial applications such as in integrated circuits. Usually it was believed that lowering sintering temperature could be achieved by adding glass flux or using starting materials with smaller particle sizes. As we known, adding glass flux usually caused detrimental effect on microwave properties of ceramics due to high intrinsic loss and easily forming second phases or crystal defects as reported elsewhere [5–7]. And now in order to reduce sintering temperature and improve sintering ability there were many other investigations of chemical processing or special methods [8–18], which were developed as alternatives to conventional solid-state reaction of mixed oxides for producing ceramics by using starting materials with smaller particle sizes. Among of all these methods of wet chemical techniques, the sol–gel was undoubtedly one of useful process for producing powders with good control over stoichiometry and homogeneity, yielding nano-sized particles and widely used in many other ceramics system [19–21]. However, there were not any reports about microwave properties of MN ceramics fabricated by aqueous sol–gel process in present literatures.

H. T. Wu (✉) · W. B. Wu · F. Yang · Y. L. Yue
School of Materials Science and Engineering,
Shandong Provincial Key Laboratory of Preparation
and Measurement of Building Materials, University of Jinan,
Jinan 250022, China
e-mail: mse_wuht@ujn.edu.cn

Y. S. Jiang
Navy Submarine Academy,
Qingdao, Shandong 266071, China

The goal of this research was to explore the capabilities of sol–gel method to synthesize nano-sized powders as precursors for the preparation of MN ceramics promisingly sintered at low temperatures. The whole process involved all complexation of aqueous metal ions by non-toxic poly functional carboxyl and avoided complex steps such as refluxing of alkoxides, resulting in less time consumption compared to other techniques. The evolution of MN phase formation originated from the gel and microwave dielectric properties of MN ceramics as a function of sintering temperatures were investigated in detail. Experimental results showed that the aqueous sol–gel process was the most effective and least expensive technique used for the preparation of MN ceramics with retaining excellent microwave properties at low sintering temperatures.

2 Experimental

Analytical-grade Nb_2O_5, K_2CO_3, $Mg(NO_3)\bullet 6H_2O$, HNO_3, citric acid (CA) and ethylene glycol (EG) were used as raw materials to synthesize the MN nanopowders as shown in Fig. 1. Firstly, the mixture of Nb_2O_5 and K_2CO_3 were co-melted at 900 °C in order to obtain K_3NbO_4 phase according to phase diagram. Subsequently, K_3NbO_4 phase was dissolved in distilled water, then the solution was set at pH ~2 to form precipitate of $Nb(OH)_5$. The whole formation process of $Nb(OH)_5$ phase could be formulated from Eqs. 1–4. Thirdly, $Nb(OH)_5$ precipitate was filtered off and washed with distilled water for six times to remove the K^+ ions and then dissolved completely in citric acid water solution by continuous magnetic stirring at 300 rpm for 15 min. Meanwhile, a stoichiometric amount of $Mg(NO_3)\bullet 6H_2O$ was added to above solution and then the solution was stirred for another 30 min. Finally, ethyl alcohol (20–40 ml) was added to as-prepared mixed solution in drops and stirred for 1 h to form a transparent and stable sol. pH of the solution was maintained in the range of 3.5–5 by adding buffering agents. The sol was heated at 80 °C–90 °C for 1 h to obtain a xerogel. The xerogel was decomposed at different temperatures ranging from 500 °C to 800 °C in a muffle furnace for crystallization and phase formation of MN powders could be formulated in Eq. 5. As-prepared powers were ball milled in a polyethylene jar for 4 h using ZrO_2 balls in ethanol medium to reduce conglobation phenomena. The powders were then mixed with polyvinyl alcohol as a binder, granulated and pressed into cylindrical disks of 10 mm diameter and about 5 mm height at a pressure of about 200 MPa. These pellets were preheated at 600 °C for 4 h to expel the binder and then sintered at selected temperatures for 2 h in air at a heating rate of 5 °C /min.

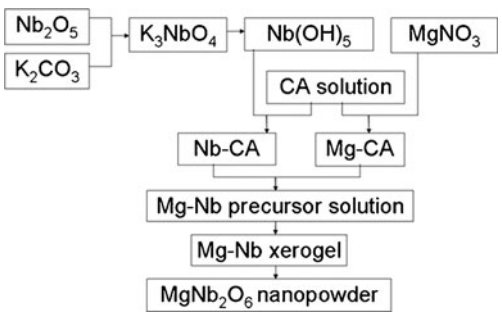

Fig. 1 Chart for the synthesis of MN nanopowders by aqueous sol–gel processing

$$3K_2CO_3 + Nb_2O_5 \rightarrow 2K_3NbO_4 + CO_2. \quad (1)$$

$$6K_3NbO_4 + 5H_2O \rightarrow 18K^+ + Nb_6O_{19}^{8-} + 10OH^-. \quad (2)$$

$$4K^+ + Nb_6O_{19}{}^{8-} + 4OH^- + 8H^+ \rightarrow K_4H_4Nb_6O_{19} \downarrow + 4H_2O. \quad (3)$$

$$K_4H_4Nb_6O_{19} + 15H^+ + 11OH^- \rightarrow 6Nb(OH)_5 \downarrow + 4K^+. \quad (4)$$

$$(-Mg - CxHyOz - Nb-) + O_2 \rightarrow MgNbO_6 + H_2O + CO_2. \quad (5)$$

In order to analyze the evolution of MN phase formation, the as-formed MN xerogel was characterized using thermogravimetry (TG) and differential thermal analysis (DTA) to study its thermal properties. Phase analysis of MN powders was conducted with the help of a Rigaku diffractometer (Model D/MAX-B, Rigaku Co., Japan) using Ni filtered CuKα radiation (λ=0.1542 nm) at 40 kV and 40 mA settings. Based on XRD analysis, raw MN powders were examined for their morphology and particle size using a transmission electron microscopy (Model JEOL JEM-2010, FEI Co., Japan). Bulk densities of sintered ceramics were measured by Archimedes method. An HP8720ES network analyzer (Hewlett-Packard, Santa Rosa, CA) was used for the measurement of microwave dielectric properties. Dielectric constants were measured using Hakki-Coleman post-resonator method by exciting TE011 resonant mode of dielectric resonator using electric probe of an antenna as suggested by Hakki and Coleman and Courtney [22]. Unloaded quality factors were measured using TE01d mode in the cavity method [23]. All measurements were made at room temperature and in the frequency of 8–10 GHz. Temperature coefficients of resonant frequency were measured in the temperature range of 25 °C–85 °C.

3 Results and discussion

Figure 2 showed TG-DTA curves of MN xerogel in pure oxygen atmosphere at a heating rate of 10 °C /min. The results indicated that obvious weight losses began at 250 °C and all chemical reactions involving weight losses, such as decomposition of organic polymeric network, finished completely below 500 °C. Total weight loss was about 80 %, which occurred in two steps: (I) initial weight loss (about 50 %) below 400 °C, resulting from the evaporation of residual solvent or water and decomposition of organic polymeric network with evolution of CO_2 and H_2O, with endothermic peaks ranging from 250 °C to 400 °C, and (ii) second weight loss (about 20–30 %) in TG curves, combined with an significantly exothermal peak in the temperature region of 400 °C–500 °C, which was attributed to the oxidation of metal-organic groups. TG results of MN xerogel were also similar with the report by sol–gel method [17].No further significant weight loss and thermometric peaks were observed above 500 °C in TG-DTA curves, indicating the minimum firing temperature to synthesize magnesium niobate phase. By comparison, DTA results mentioned by other solid-state methods [13, 14] meant different MN formation temperatures, all of which were above 500 °C.

XRD patterns of MN xerogel calcined in oxygen atmosphere ranging from 500 °C to 800 °C for 30 min were shown in Fig. 3. It was pleasantly found that the crystallization of MN phase took place obviously at 500 °C, this phenomenon was recognized from the exothermic peak of DTA and corresponding TG profile as described above. The xerogel fired at 500 °C consisted of predominant peaks of $MgNb_2O_6$ matching with JCPDS file number 33–0875, also free from any second phases such as $Mg_5Nb_4O_{15}$ or $Mg_4Nb_2O_9$. In the temperature region from 600 °C to 800 °C, the intensity of MN peaks was gradually enhanced and no second phases were found all the time. XRD results indicated that calcination temperature of synthesizing pure MN phase was remarkably decreased to 500 °C by aqueous

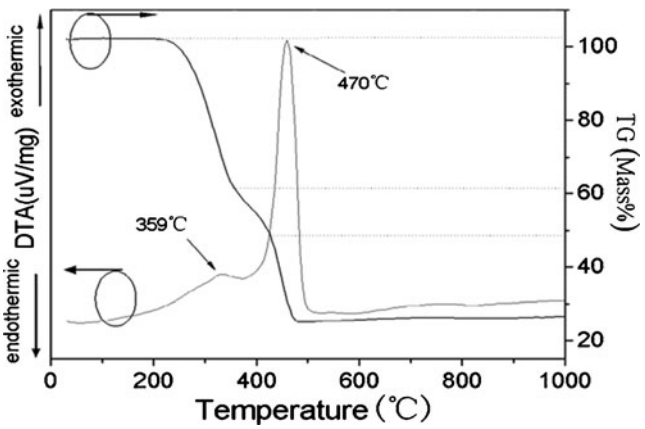

Fig. 2 TG-DTA curves of the MN xerogel in oxygen atmosphere

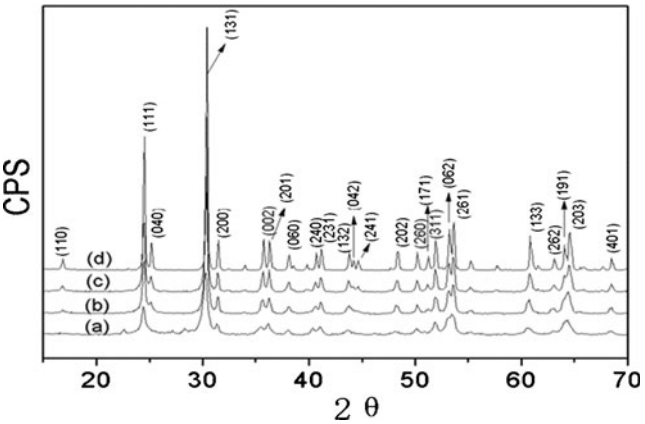

Fig. 3 X-ray diffraction patterns of the MN xerogel calcined at (*a*) 500 °C, (*b*)600 °C, (*c*)700 °C, (*d*)800 °C for 30 min

sol–gel method, which showed obvious advantage in comparison to these of conventional mixed oxide route reported before [13, 14] and other chemical methods [8–12, 16–18] as shown in Table 1.

The TEM micrograph of MN nanopowders calcined at 500 °C was illustrated in Fig. 4. As observed in the image, it was worth noting that particles were slightly agglomerated due to high surface to volume ratio and basically regular in shape. Particle sizes were measured by liner intercept method [24] with the range of about 20–40 nm. For comparison, MN particle sizes synthesized by different methods were also listed in Table 1 and the results showed that MN powders had smaller particle size of 20–40 nm by aqueous sol–gel process with larger surface area and free energy. Since surface free energy is considered to be a driving force in the sintering process, a number of sintering models have been researched for the initial stage of sintering and the resulting equation has been deduced. According to sintering equation of initial stage [25], the use of MN nanopowders as starting materials was effective in preparing high density MN ceramics promisingly through low-temperature sintering and short sintering time. Therefore, the sol–gel process showed significant advantages of sintering ceramics at relatively low temperatures, which had been demonstrated by many other reports.

Sintering characteristics of samples depending on sintering temperatures were plotted in Fig. 5. Figure 5 represented curves of apparent densities and diametric shrinkage ratio of MN ceramics as a function of sintering temperature, through which the optimized sintering temperature was determined. Relative densities increased from nearly 80 % to 95 % as the sintering temperature increased from 1050 °C to 1150 °C. A saturated value of relative densities was obtained at 1150 °C. The curve of diametric shrinkage ratio showed the similar tendency and also increased with the increase of sintering temperatures, and then saturated at about 1150 °C. SEM micrographs of MN ceramics sintered at different temperatures for 2 h were illustrated in Fig. 6(a–e). Changes in

Table 1 Comparison of $MgNb_2O_6$ powders synthesized by different methods

Process	Calcination temperature (°C)	Grain size(nm)	Reference
Precipitation	750/750	50/100–300	[8, 9]
Wet-Chemical	800	70	[10]
Molten Salt	1100	3000–5000	[11]
High-Energy Ball Milling	700	1000	[12]
Solid-State Reaction	1000/1150/1250	125~780/3000/-	[13–15]
Citrate Gel	700	80/90	[16, 17]
Polymerized Complex	900	170	[18]
Aqueous Sol–gel	500	20–40	Our results

"-" denoted that no values of grain size were mentioned

porosity and grain size could be seen with an increase of sintering temperature. Apparent porosity decreased as sintering temperature increased from 1050 °C to 1150 °C and all pores almost disappeared at 1150 °C on the surface of MN samples. While sintered at 1250 °C, the molten phenomenon of MN grains was found as shown in Fig. 6(e) due to exceedingly high sintering temperatures. In addition, the morphology of MN ceramics exhibited large lath-shaped grains and nearly spherical particles dispersed around large grains,which was similar with other reports[26, 27]. Based on SEM results of MN samples, it was shown that MN ceramics were successfully prepared with high density through the sol–gel process at 1150 °C and sintering temperature was reduced significantly compared to solid-state reaction method [2, 4].

Plots of ε_r, $Q\times f$ and τ_f values were shown in Fig. 7 as a function of sintering temperatures. ε_r values of MN ceramics steadily increased from 14.3 to 18.7 as sintering temperatures ranged from 1050 °C to 1150 °C. Based on SEM results of microstructures as shown in Fig. 6(a–c), it was obvious that low ε_r values were caused by undense microstructure of MN ceramics with much pores at sintering temperatures <1150 °C. ε_r values were approximately saturated about 18.7 at sintering temperatures >1150 °C. The curve of ε_r values showed a similar tendency with those of apparent density and shrinkage ratio, which were sensitive to dense degree of ceramics significantly. In general, higher density could achieve higher dielectric constant owing to a lower amount of pores (ε_r~1). In addition, due to free from $Mg_5Nb_4O_{15}$ or $Mg_4Nb_2O_9$ phase the effect on dielectric constants caused by second phase could be negligible. The results of ε_r values obtained at 1150 °C by sol–gel process were comparable with these results sintered at 1400 °C by solid-state reaction method [2, 4].

With increasing sintering temperatures from 1050 °C to 1250 °C, $Q\times f$ values increased from 22,365 GHz to 91,000 GHz with saturated $Q\times f$ values ~90,000 GHz in the sintering temperature region of 1150 °C–1250 °C. Remarkable increase in $Q\times f$ values ranging from 1050 °C to 1150 °C was also related to the reduction of porosity according to SEM results of microstructures as shown in Fig. 6(a–c). Relative density was important factor in controlling dielectric loss, which had been shown on many other microwave dielectric materials. Due to increased density $MgNb_2O_6$ ceramics sintered at 1150 °C had the excellent $Q\times f$ value of 90,700 GHz, which was comparable with the results of $Q\times f$~91,500 GHz

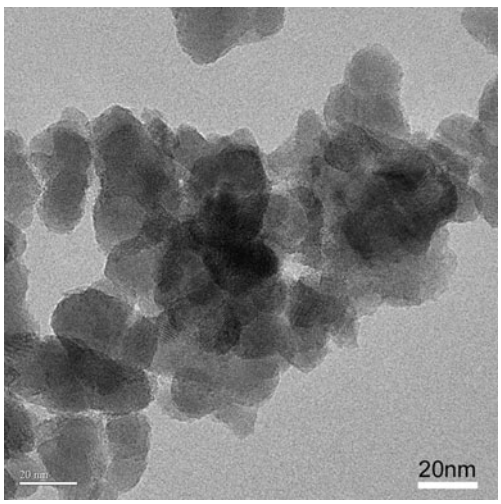

Fig. 4 TEM micrograph of the raw MN nanopowders calcined at 500 °C for 30 min

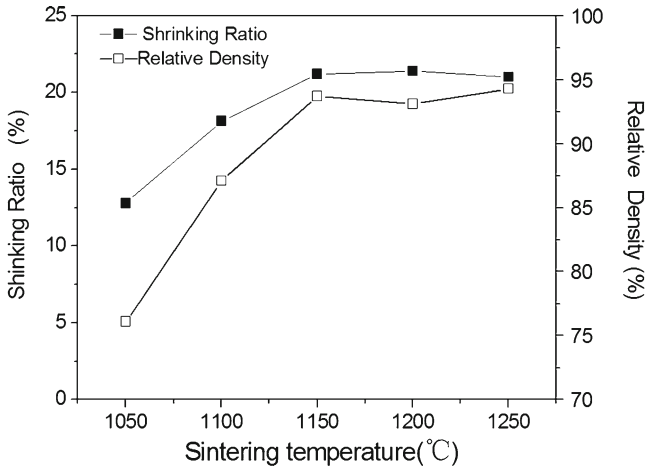

Fig. 5 Relative densities and shrinkaging ratio of MN ceramics as a function of sintering temperatures

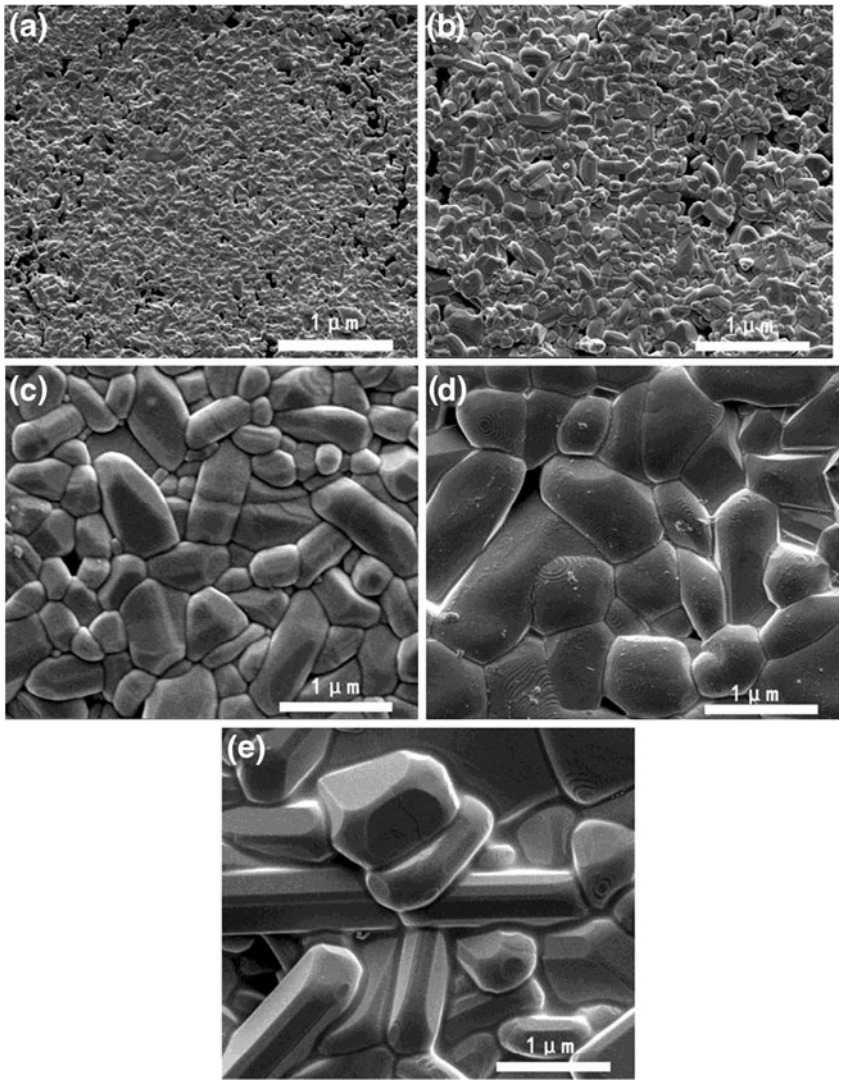

Fig. 6 FE-SEM micrographs of MN ceramics sintered at different sintering temperature for 2 h ((**a**)~(**e**) corresponding to 1050 °C, 1100 °C,1150 ° C,1200 °C, 1250 °C)

while sintered at 1450 °C by solid-state methods [2, 4]. Moreover, remarkable variations in τ_f values of MN ceramics were not recognized with sintering temperatures from 1050 °C to 1250 °C and these values ranged from −40 to −60 ppm/°C. Thus, it was considered that additional improvement in τ_f value was required for dielectric resonator applications at high frequency.

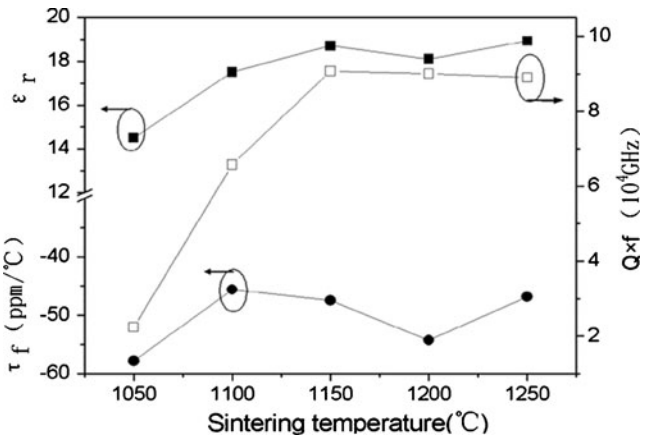

Fig. 7 Curves of ε_r, $Q\times f$ and τ_f values as a function of the sintering temperatures for MN ceramics in the temperature region of 1150 °C–1250 °C

4 Conclusions

The aqueous sol–gel synthetic route was efficiently used to prepare columbite-structure $MgNb_2O_6$ powders with particle sizes of nearly 20–40 nm, which showed major advantages over other methods reported before. A considerable decrease in calcinations temperature (at 500 °C) was obtained in pure oxygen atmosphere for the formation of $MgNb_2O_6$ nanopowders. Moreover, sintering ability and microwave properties of $MgNb_2O_6$ ceramics were systematically investigated at different sintering temperatures. $MgNb_2O_6$ samples with nearly full densities were obtained at 1150 °C and showed excellent microwave dielectric properties of ε_r=18.7, $Q\times f$=

90,700 GHz and τ_f=−48.5 ppm/°C. Experimental results showed that the aqueous sol–gel process could achieve nano-sized powders with larger surface area and high free energy, which was beneficial to reduce sintering temperature and optimize the performance of $MgNb_2O_6$ ceramics.

Acknowledgments This work was supported by Natural Science Youth Foundation of Shandong Province (No. ZR2011EMQ005) and National Natural Science Foundation (No.51172093, 51042009).

References

1. H. Ohsato, J. Ceram. Soc. Jpn. **113**, 703 (2005)
2. C.F. Yang, C.C. Chan, C.M. Cheng, Y.C. Chen, J. Eur. Ceram. Soc. **25**, 2849 (2005)
3. W.C. Tzou, Y.C. Chen, C.F. Yang, C.M. Cheng, Mater. Res. Bull. **41**, 1357 (2006)
4. C.M. Cheng, Y.C. Chen, C.F. Yang, C.C. Chan, J .Electroceram. **18**, 155 (2007)
5. W.S. Xia, L.X. Li, P. Zhang, P.F. Ning, Mater. Lett. **65**, 3317 (2011)
6. K.W. Tay, Y.P. Fu, J.F. Huang, H.C. Huang, Ceram. Int. **37**, 1025 (2011)
7. H.T. Wu, L.X. Li, J. Sol–gel Sci. Technol. **58**, 48 (2011)
8. S.C. Navale, A.B. Gaikwad, V. Ravi, Mater. Res. Bull. **41**, 1353 (2006)
9. L. Srisombat, S. Ananta, S. Phanichphant, Mater. Lett. **58**, 853 (2004)
10. L.P.S. Santos, E.R. Camargo, M.T. Fabbro, E. Longo, E.R. Leite, Ceram. Int. **33**, 1205 (2007)
11. V. Shanker, A.K. Ganguli, Bull. Mater. Sci. **26**, 741 (2003)
12. L.B. Kong, J. Ma, H. Huang, R.F. Zhang, J. Alloys Compd. **340**, L1 (2002)
13. S. Ananta, Mater. Lett. **58**, 2781 (2004)
14. N.K. Kim, Mater. Lett. **32**, 127 (1997)
15. S. Ananta, R. Brydson, N.W. Thomas, J. Eur. Ceram. Soc. **19**, 355 (1999)
16. R. Pasricha, V. Ravi, Mater. Lett. **59**, 2146 (2005)
17. Y.C. Zhang, X.N. Zhou, X. Wang, J. Sol–gel Sci. Technol. **50**, 348 (2009)
18. E.R. Camargo, E. Longo, E.R. Leite, J. Sol–gel Sci. Technol. **17**, 111 (2000)
19. Y.D. Hou, L. Hou, J.L. Zhao, M.K. Zhu, H. Yan, J. Electroceram. **26**, 37 (2011)
20. Z.Y. Wen, X.X. Xu, J.X. Li, J. Electroceram. **22**, 342 (2009)
21. C.-S. Hong, H.-H. Park, H.-H. Park, H.J. Chang, J .Electroceram. **22**, 353 (2009)
22. B.W. Hakki, P.D. Coleman, IEEE Trans. **8**, 116 (1960)
23. W.E. Courtney, IEEE Trans. **18**, 476 (1970)
24. A. Thorvaldsen, Acta. Mater. **45**, 595 (1997)
25. S.-J.L. Kang, *Sintering: Densification, Grain Growth & Microstructure* (Elsevier Butterworth-Heinemann, Burlington, 2005), pp. 50–55
26. C.L. Huang, K.H. Chiang, Mat. Sci. Eng. A-Struct. **474**, 243 (2008)
27. C.S. Hsu, C.L. Huang, J.F. Tseng, C.Y. Huang, Mater. Res. Bull. **38**, 1091 (2003)